Supplementary Information

Specifically targeting mixed-type dimeric G-quadruplexes by berberine dimers

Zi-Qi Li, Ting-Cong Liao, Cheng Dong, Jian-Wei Yang, Xiao-Jie Chen, Lihong Liu, Yuan Luo, Yuan-Yuan Liang, Wen-Hua Chen,* Chun-Qiong Zhou*

Guangdong Provincial Key Laboratory of New Drug Screening, School of Pharmaceutical Sciences, Southern Medical University, Guangzhou 510515, China, E-mail: whchen@smu.edu. cn, zcqlg@smu.edu.cn

Figure Legend

Experimental details

Materials, methods and instrumentation. ^{1}H and ^{13}C NMR spectra were recorded in DMSO-d_6 on a Varian Mercury 400 spectrometer. ESI-MS and HR-ESI-MS spectra were measured on Waters UPLC/Quattro Premier XE and Agilent 6460 Triple Quadrupole mass spectrometers, respectively. Compounds **1b**, **1c**, **2** and **3** were prepared according to reported protocols.[1-2]

Synthesis of compound 1a. To a solution of berberrubine **2** (107 mg, 0.3 mmol) in MeCN (20 mL) was added diethylene glycol ditosylate **3** (62 mg, 0.15 mmol). The resulting mixture was refluxed for 84 h, and then concentrated under reduced pressure. The obtained residue was subjected to anion exchange into chloride form, and subsequently purified by chromatography on a reverse-phase column, eluted with a gradient of methanol in water (0–10%), to give compound **1a** (93 mg, 79%) as a yellow powder having ^{1}H NMR (400 MHz, d_6-DMSO) δ 9.63 (s, 2H), 8.80 (s, 2H), 8.10 (d, J = 9.0 Hz, 2H), 7.92 (d, J = 9.0 Hz, 2H), 7.40 (s, 2H), 7.05 (s, 2H), 6.13 (s, 4H), 4.95 (s, 4H), 4.27 (s, 4H), 3.92 (s, 6H), 3.89 (s, 4H), 3.15 (s, 4H); ^{13}C NMR (100 MHz, d_6-DMSO) δ 150.6, 150.1, 147.9, 145.6, 143.0, 137.4, 133.2, 130.6, 126.5, 124.0, 122.3, 120.6, 120.4, 108.6, 105.5, 102.5, 73.2, 69.9, 57.2, 55.4, 26.6; ESI-MS *m/z*: 357.7 ([M-2Cl]$^{2+}$) and HRMS for $C_{42}H_{38}N_2O_9^{2+}$ ([M-2Cl]$^{2+}$) Calcd: 357.1283, found: 357.1282.

References:

1 C. -Q. Zhou, J. -W. Yang, C. Dong, Y. -M. Wang, B. Sun, J. -X. Chen, Y. -S. Xu and W. -H. Chen, *Org. Biomol. Chem*., 2016, **14**, 191.

2 Y. -M. Wang, C. -Q. Zhou, J. -X. Chen, Y. -L. Lin, W. Zeng, B. -C. Kuang, W. -L. Fu and W. -H. Chen, *Med. Chem. Commun*., 2013, **4**, 1400.

Table

Table S1. G2T1 binding constants (K's, M^{-1}), stabilization temperatures ($\Delta T_{m,}$ °C), and binding

ratio and mode of previously reported binders.

Binder	K	ΔT_m	Binding ratio and mode	DNA structure	Ref.
Triaryl-imidazole	1.28×10^5	23	1:1, pocket intercalation	Mixed-type	[1]
Dinickel-salphen	3.11×10^7	14.1	2:1, End-stacking	Antiparallel	[2]
Cyclic helicene	2.31×10^6	/	3:1, pocket intercalation	Mixed-type	[3]
QATPE [a]	8.94×10^6	6.6	4:1, pocket intercalation and end-stacking	Mixed-type	[4]
TMPipEOPP [b]	$0.6\sim2.5\times10^6$	9.1~13	1:1.6, pocket intercalation and end-stacking	Mixed-type	[5, 6]
DR4-47 [c]	/	>28.5	/, End-stacking	Mixed-type	[7]
EPI [d]	2.60×10^7	/	2:1, /	Mixed-type	[8]
Ni-M [e]	4.6×10^7	12	1:1, End-stacking	Antiparallel	[9]
TMPyP4 [b]	2.4×10^6	/	4:1, External and end-stacking	Mixed-type	[10]
Azatrux [f]	1.1×10^6	/	2.8:1, pocket intercalation and end-stacking	Mixed-type	[10]

[a] QATPE = 1, 1, 2, 2-Tetrakis{4-[(trimethylammonium)butoxy]phenyl}tetraphenylethene tetrabromide; [b] TMPyP4 and TMPipEOPP, = cationic porphyrin and its derivative; [c] DR4-47 = Hybrid oxazole-triazole ligand; [d] EPI = epiberberine; [e] Ni-M = Zinc-finger like nanosized chiral Ni(II)-supramolecular complex; [f] Azatrux = three side-chained triazatruxene derivative azatrux; / = no detected.

References:

1 M. -H. Hu, S. -B. Chen, B. Wang, T. -M. Ou, L. -Q. Gu, J. -H. Tan and Z. -S. Huang, *Nucleic Acids Res.*, 2017, **45**, 1606.

2 C. -Q. Zhou, T. -C. Liao, Z. -Q. Li, J. Gonzalez-Garcia, M. Reynolds, M. Zou and R. Vilar, *Chem. Eur. J.*, 2017, **23**, 4713.

3 K. Shinohara, Y. Sannohe, S. Kaieda, K. Tanaka, H. Osuga, H. Tahara, Y. Xu, T. Kawase, T. Bando and H. Sugiyama, *J. Am. Chem. Soc.*, 2010, **132**, 3778.

4 Q. Zhang, Y. -C. Liu, D. -M. Kong and D. -S. Guo, *Chem. Eur. J.*, 2015, **21**, 13253.

5 X. -X. Huang, L. -N. Zhu, B. Wu, Y. -F. Huo, N. -N. Duan and D. -M. Kong, *Nucleic Acids Res.*, 2014, **42**, 8719.

6 L. -N. Zhu, B. Wu and D. -M. Kong, *Nucleic Acids Res.*, 2013, **41**, 4324.

7 A. R. O. Cousins, D. Ritson, P. Sharma, M. F. G. Stevens, J. E. Moses and M. S. Searle, *Chem. Commun.*, 2014, **50**, 15202.

8 L. Zhang, H. Liu, Y. Shao, C. Lin, H. Jia, G. Chen, D. Yang and Y. Wang, *Anal. Chem.*, 2015, **87**, 730.

9 C. Q. Zhao, L. Wu, J. S. Ren, Y. Xu and X. Qu, *J. Am. Chem. Soc.*, 2013, **135**, 18786.

10 A. Cummaro, L. Fotticchia, M. Franceschin, C. Giancola and L. Petraccone, *Biochimie* 2011, **93**, 1392.

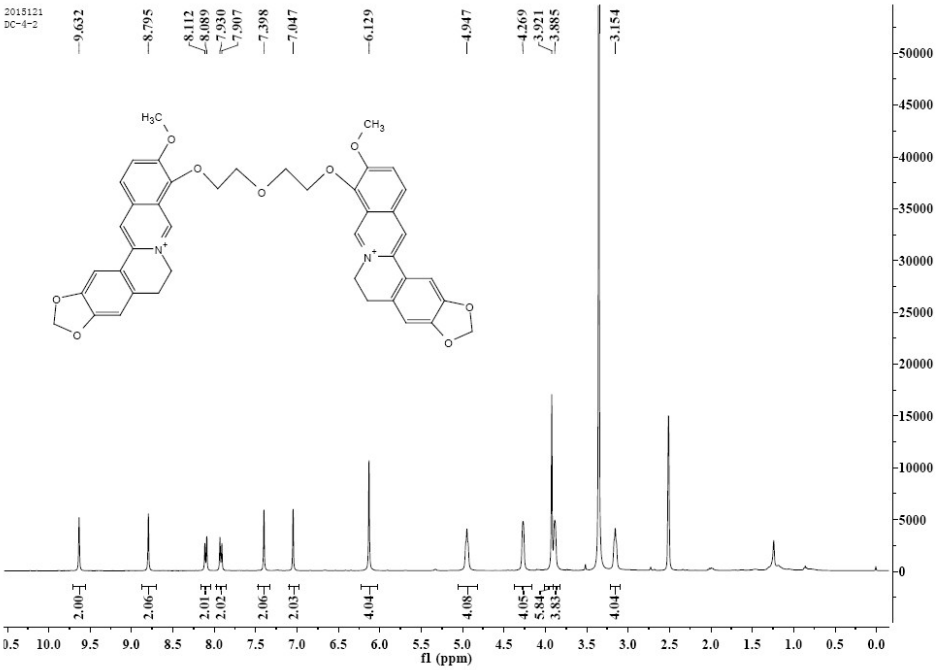

Fig. S1 ^{1}H NMR (400 MHz) of compound **1a** in d_6-DMSO.

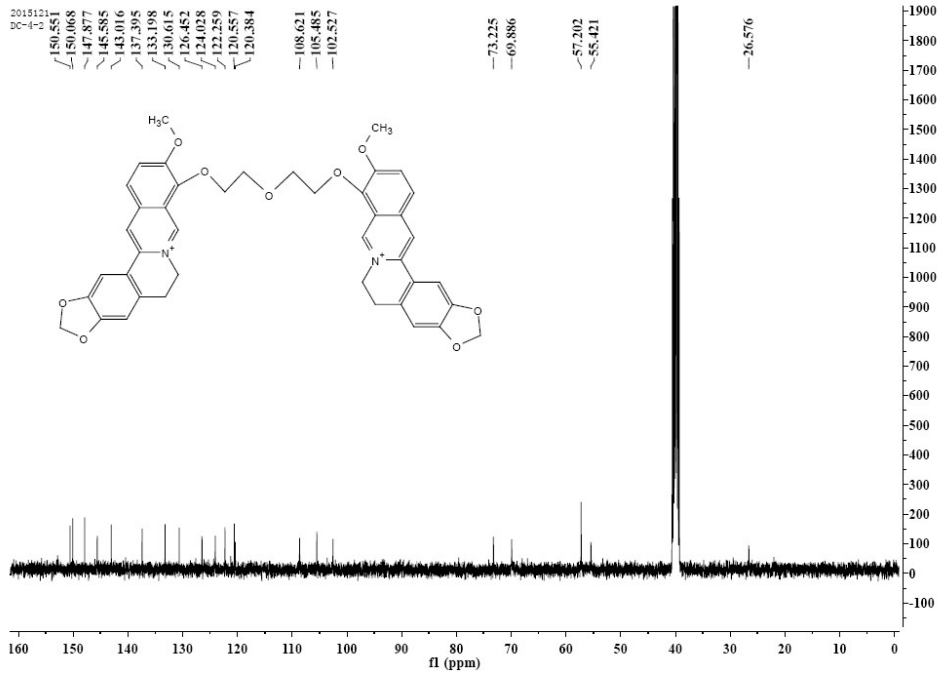

Fig. S2 ^{13}C NMR (100 MHz) of compound **1a** in d_6-DMSO.

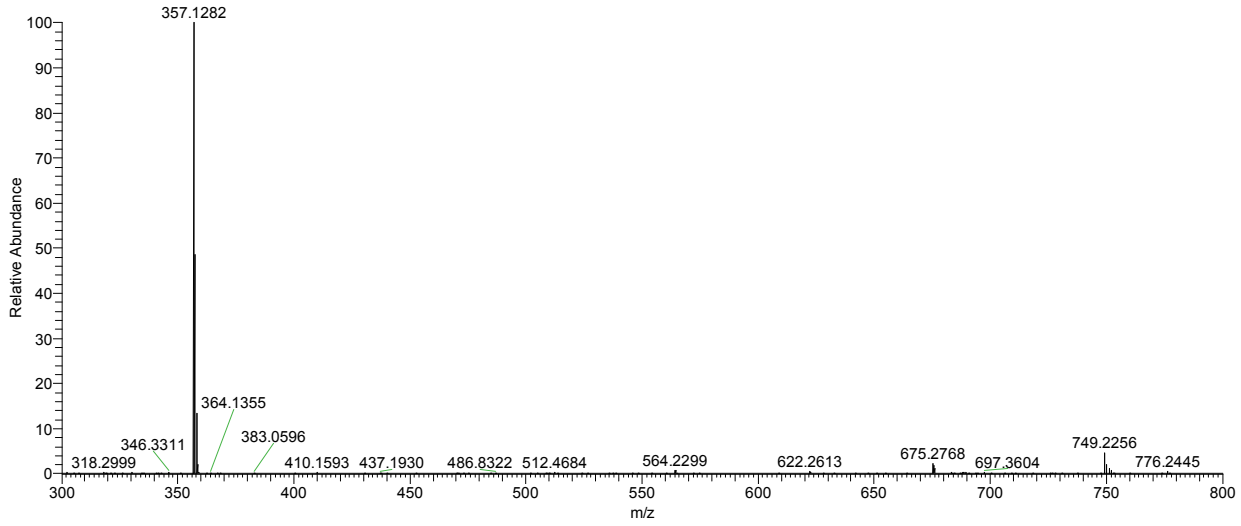

Fig. S3 HR-ESI-MS of compound **1a**.

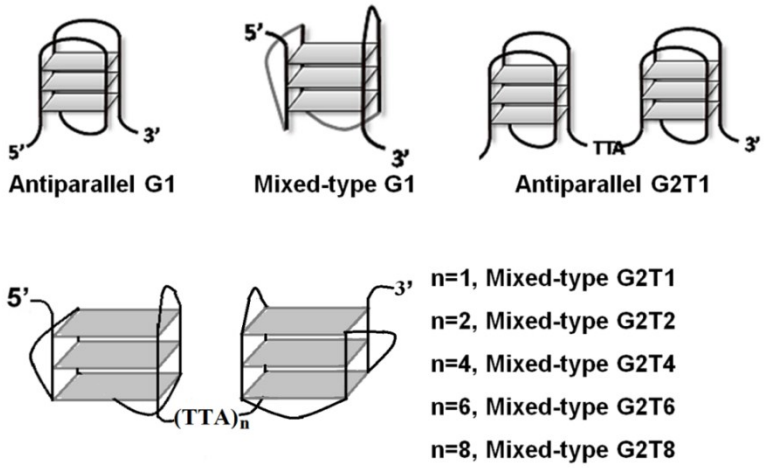

Fig. S4 Schematic representation of various monomeric and dimeric G-quadruplexes.

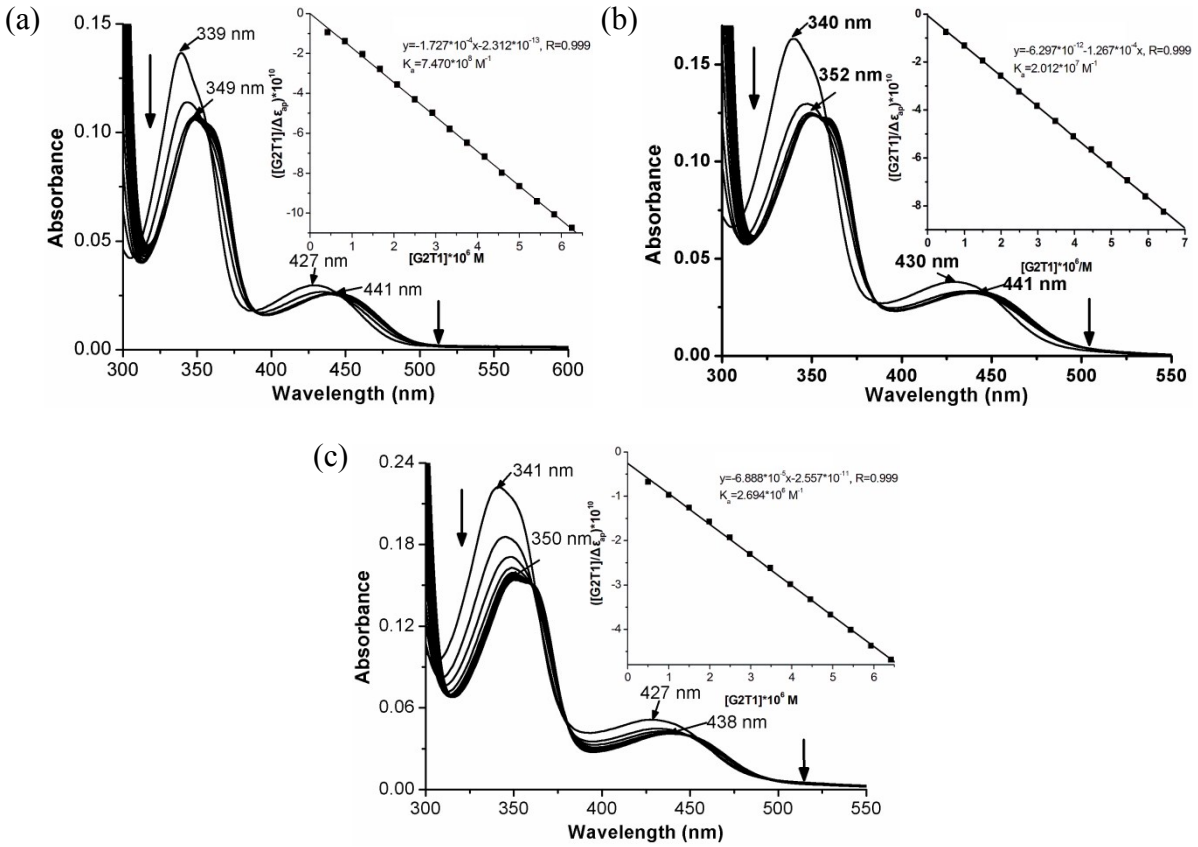

Fig. S5 UV-Vis titration of 5 μM compounds **1a** (a), **1b** (b) and **1c** (c) with mixed-type G2T1 DNA of increasing concentrations (0~6.50 μM) in 10 mM Tris-HCl, 100 mM KCl and pH 7.0. Inset: a reciprocal plot of $([G2T1]/\Delta\varepsilon_{ap})\times10^{10}$ *versus* $[G2T1]\times10^{6}$, $\Delta\varepsilon_{ap}=(A_{observed}-A_{free\ compound})/[compound]$.

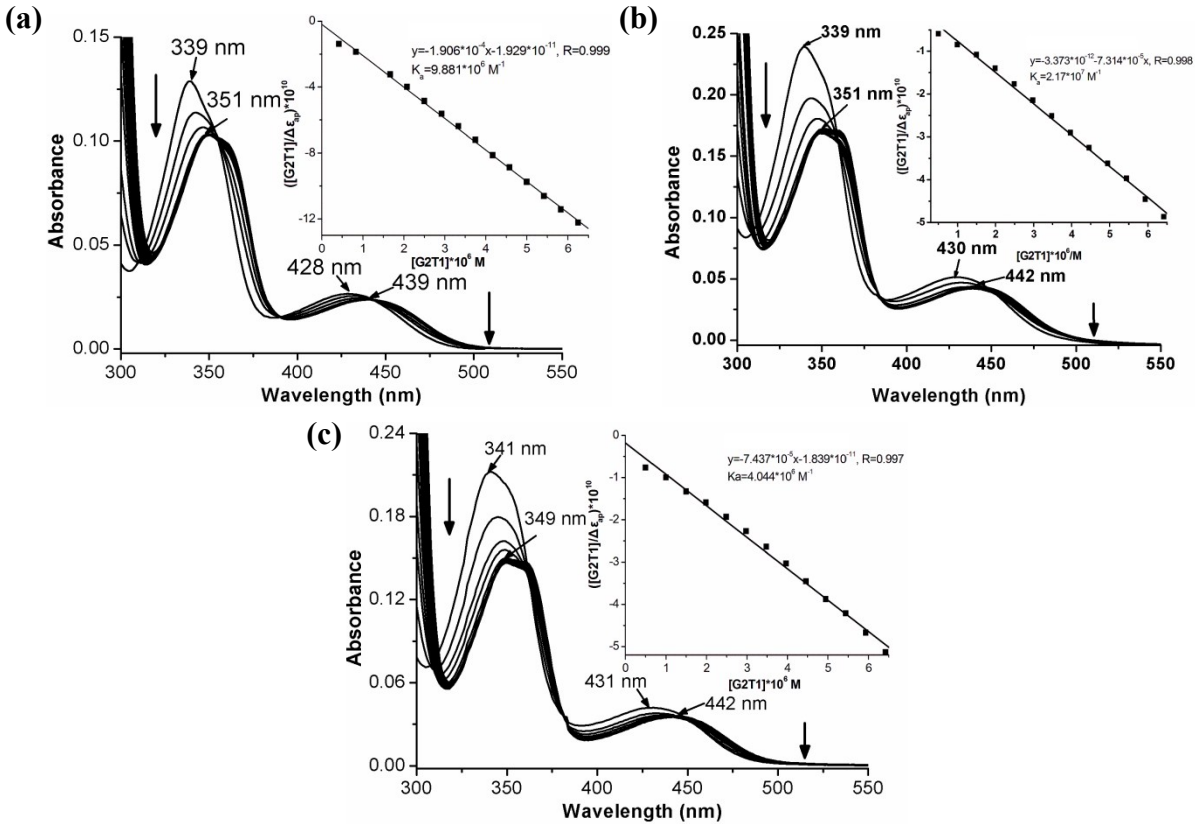

Fig. S6 UV-Vis titration of 5 μM compounds **1a** (a), **1b** (b) and **1c** (c) with antiparallel G2T1 DNA of increasing concentrations (0~6.50 μM) in 10 mM Tris-HCl, 100 mM NaCl and pH 7.0. Inset: a reciprocal plot of $([G2T1]/\Delta\varepsilon_{ap})\times10^{10}$ *versus* $[G2T1]\times10^{6}$, $\Delta\varepsilon_{ap}=(A_{observed}-A_{free\ compound})/[compound]$.

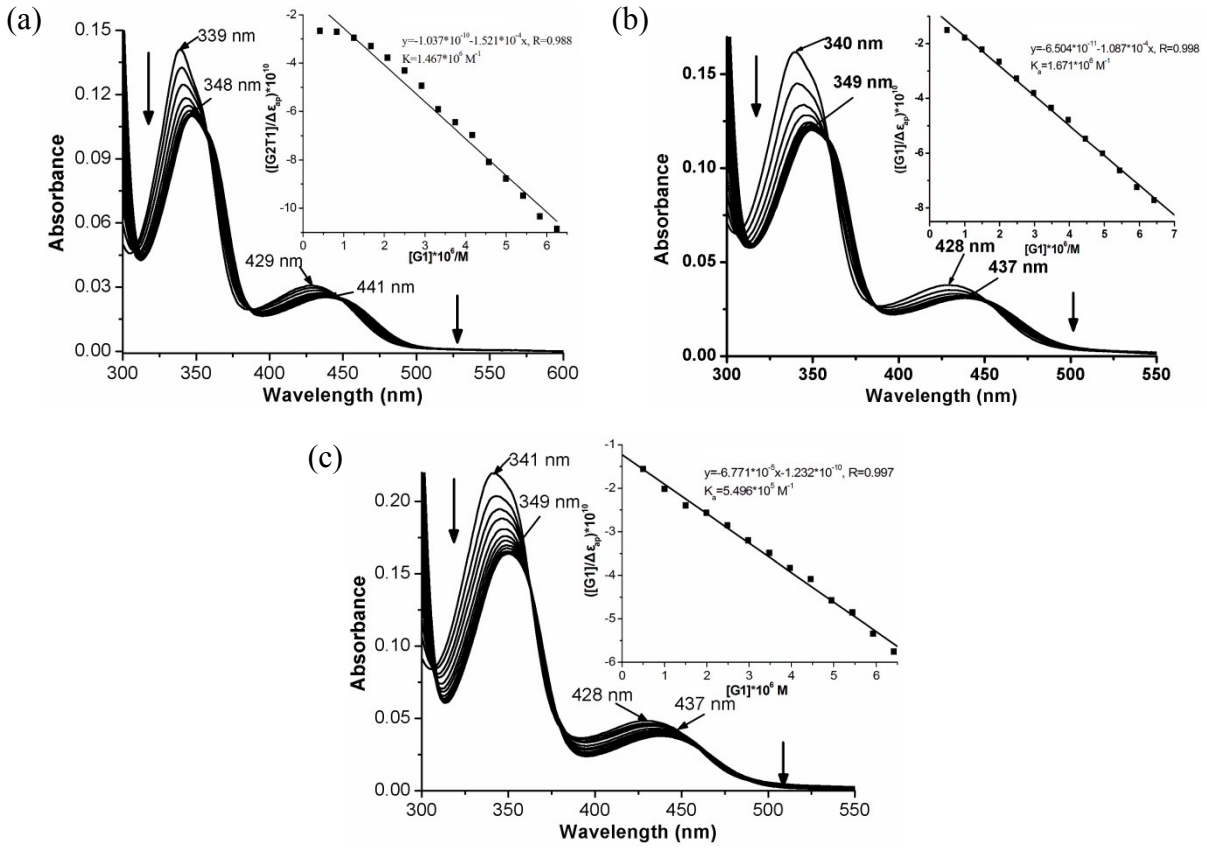

Fig. S7 UV-Vis titration of 5 μM compounds **1a** (a), **1b** (b) and **1c** (c) with mixed-type G1 DNA of increasing concentrations (0~6.50 μM) in 10 mM Tris-HCl, 100 mM KCl and pH 7.0. Inset: a reciprocal plot of $([G1]/\Delta\varepsilon_{ap})\times10^{10}$ *versus* $[G1]\times10^{6}$, $\Delta\varepsilon_{ap} = (A_{observed}-A_{free\ compound}) / [compound]$.

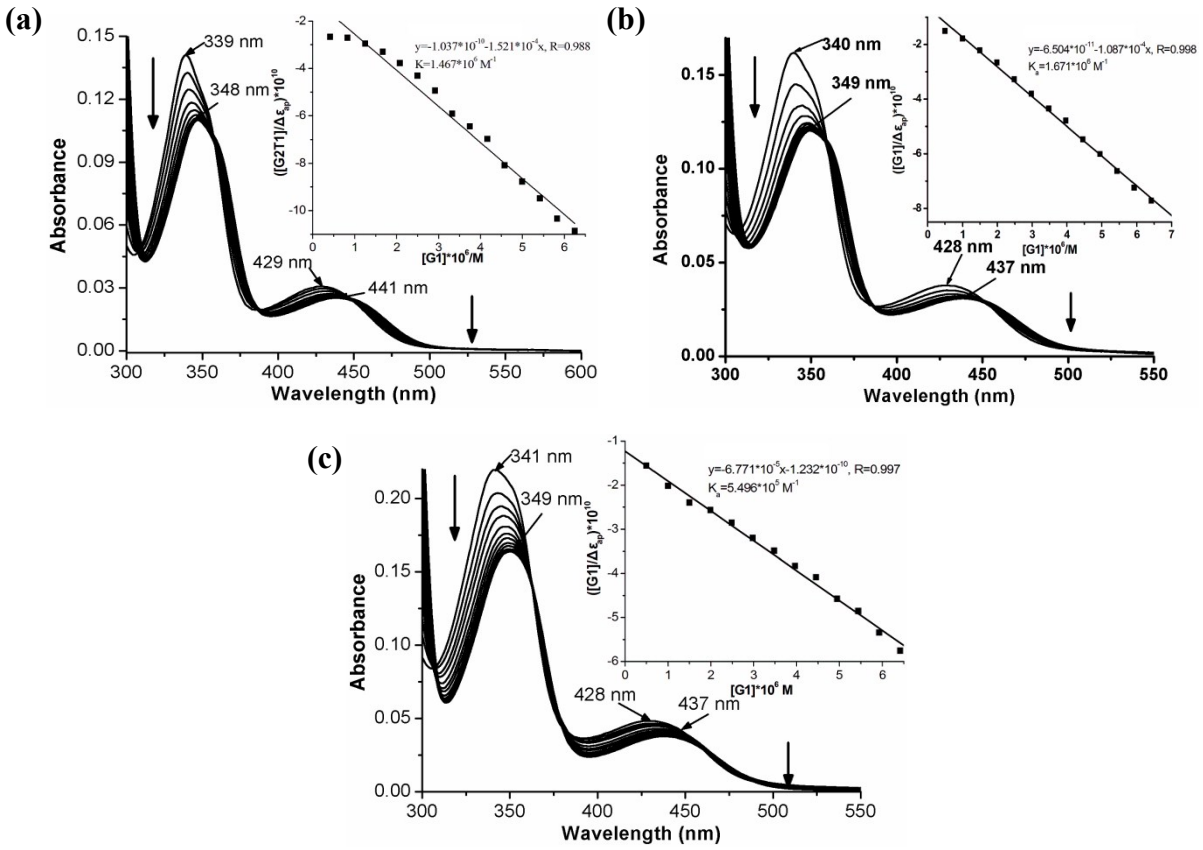

Fig. S8 UV-Vis titration of 5 μM compounds **1a** (a), **1b** (b) and **1c** (c) with antiparallel G1 DNA of increasing concentrations (0~6.50 μM) in 10 mM Tris-HCl, 100 mM NaCl and pH 7.0. Inset: a reciprocal plot of $([G1]/\Delta\varepsilon_{ap})\times10^{10}$ *versus* $[G1]\times10^{6}$, $\Delta\varepsilon_{ap}=(A_{observed}-A_{free\ compound})$ /[compound].

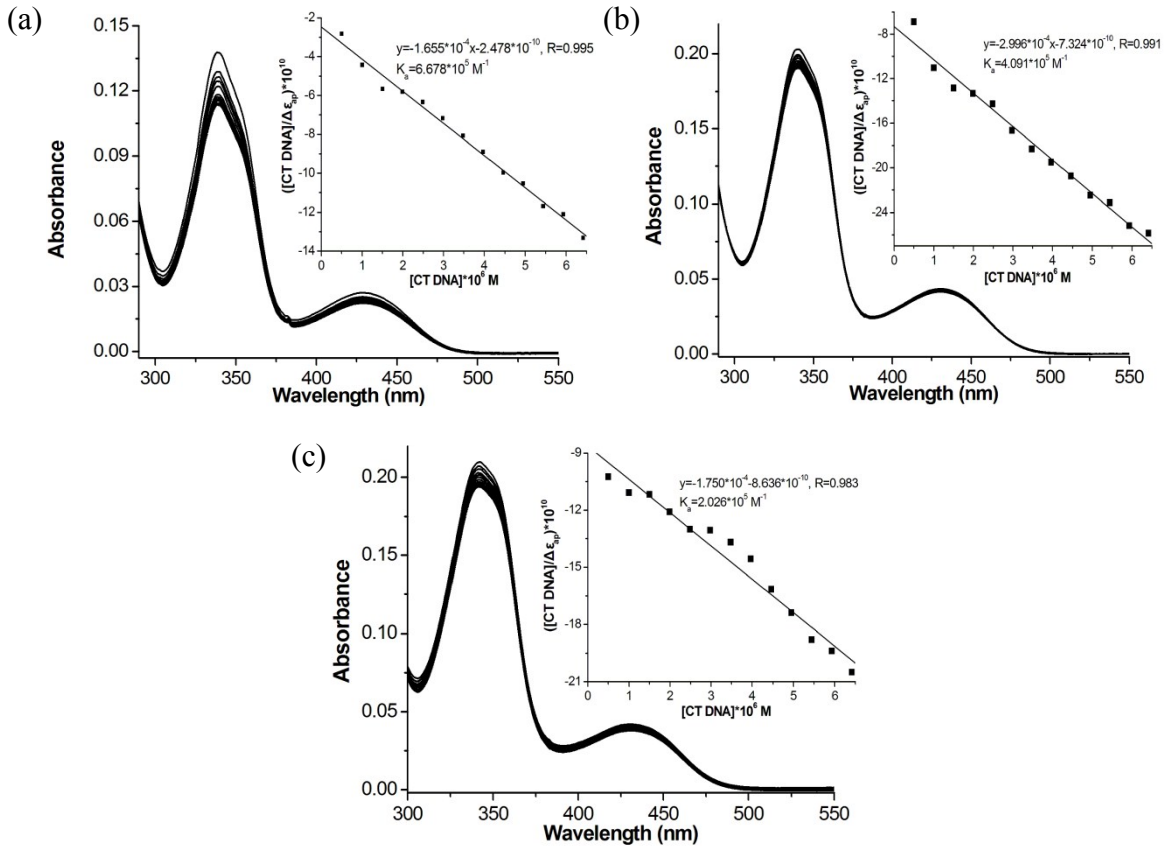

Fig. S9 UV-Vis titration of 5 μM compounds **1a** (a), **1b** (b) and **1c** (c) with CT DNA of increasing concentrations (0~6.50 μM) in 10 mM Tris-HCl, 100 mM NaCl and pH 7.0. Inset: a reciprocal plot of ([CT DNA]/$\Delta\varepsilon_{ap}$)×10^{10} *versus* [CT DNA] ×10^6, $\Delta\varepsilon_{ap}$ = ($A_{observed}$–$A_{free\ compound}$)/[compound].

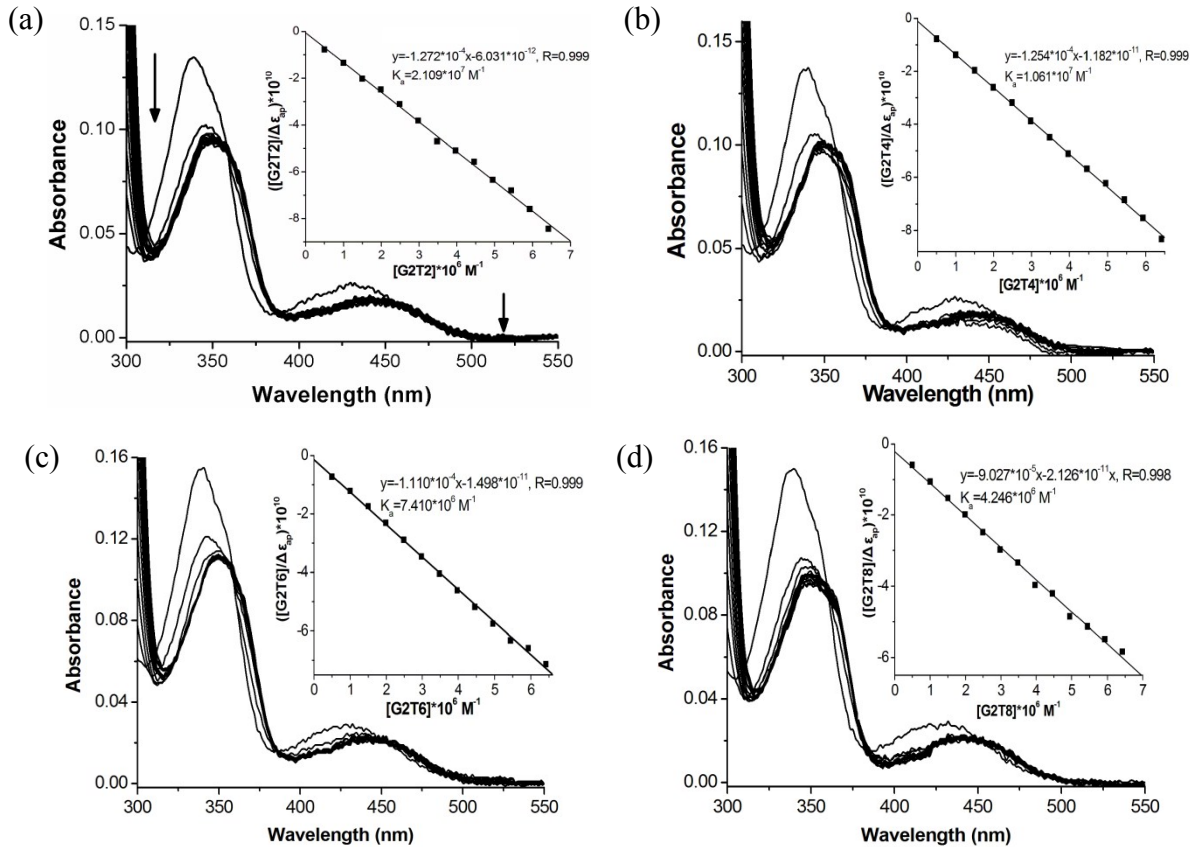

Fig. S10 UV-Vis titration of compound **1a** (5 μM) with mixed-type G2T2 (a), G2T4 (b), G2T6 (c) and G2T8 (d) of increasing concentrations (0~6.50 μM) in 10 mM Tris-HCl, 100 mM KCl and pH 7.0. Inset: a reciprocal plot of $([DNA]/\Delta\varepsilon_{ap})\times10^{10}$ *versus* $[DNA]\times10^{6}$, $\Delta\varepsilon_{ap} = (A_{observed} - A_{free\ compound}) / [compound]$.

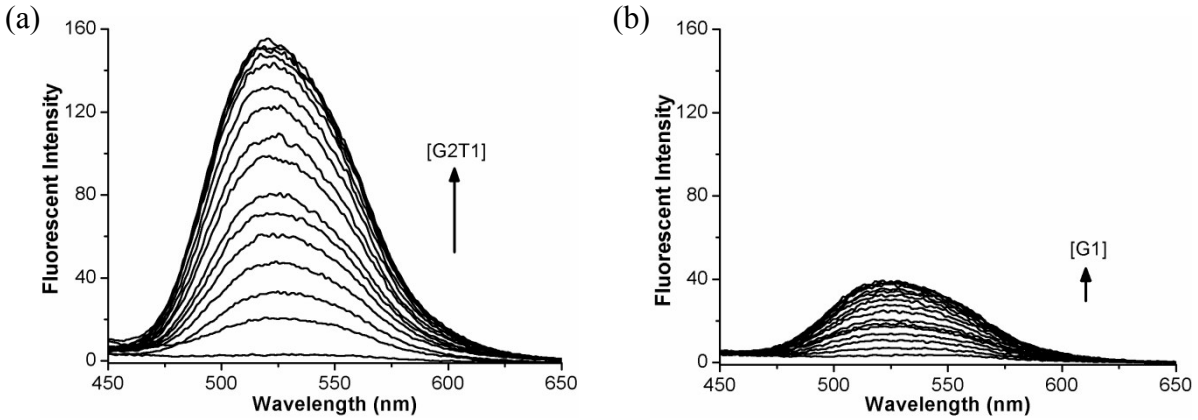

Fig. S11 Fluorescent spectra of compound **1b** (0.5 μM) in the presence of mixed-type G2T1 (a) and G1 (b) of varying concentrations (0~0.85 μM), in 10 mM Tris-HCl and 100 mM KCl (pH 7.0) at λ_{ex}=350 nm。

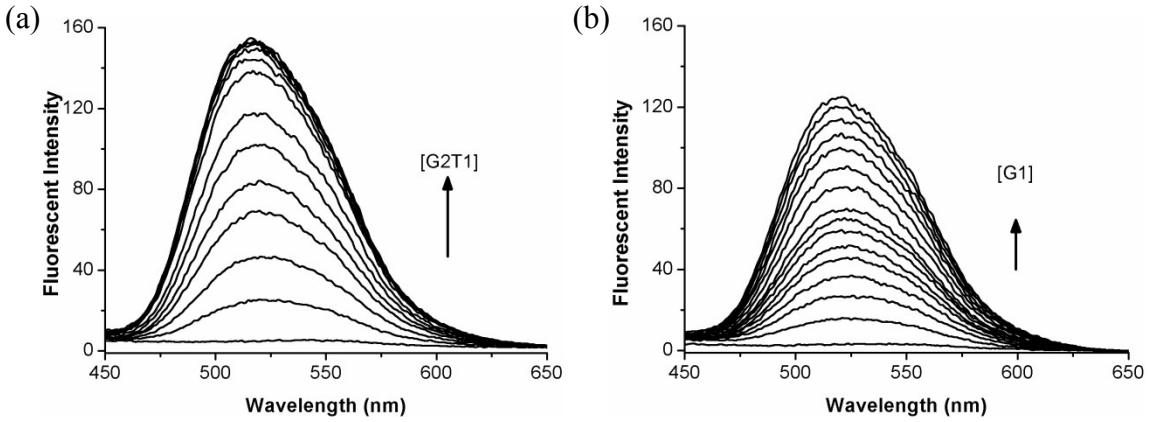

Fig. S12 Fluorescent spectra of compound **1c** (0.5 μM) in the presence of different concentration mixed-type G2T1 (a) and G1 (b) of varying concentrations (0~0.85 μM), in 10 mM Tris-HCl and 100 mM KCl (pH 7.0) at λ_{ex}=350 nm。

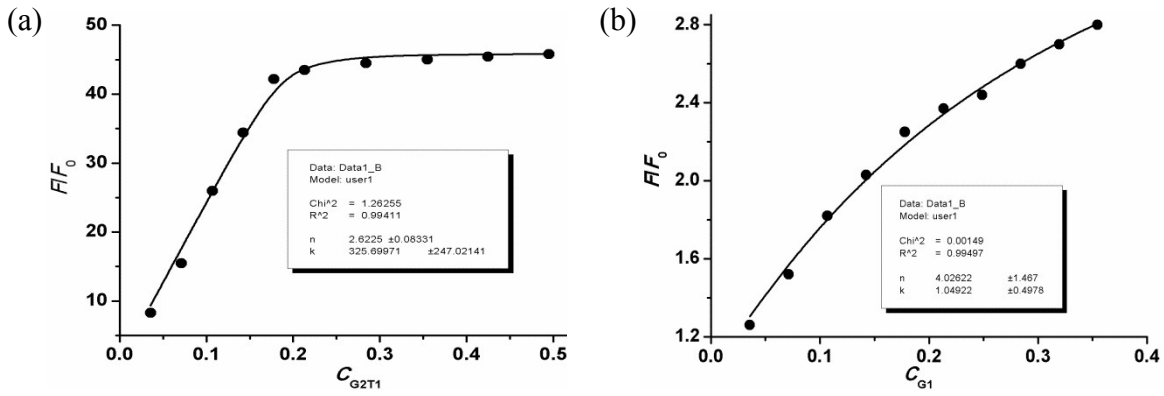

Fig. S13 Plot of the relative fluorescent intensity (F/F_0) of compound **1a** (0.5 μM) against the concentrations of mixed-type G2T1 (a) and mixed-type G_1 (b) in 10 mM Tris-HCl buffer (100 mM KCl, pH 7.0). $\lambda_{ex}/\lambda_{em}$ = 355/530 nm.

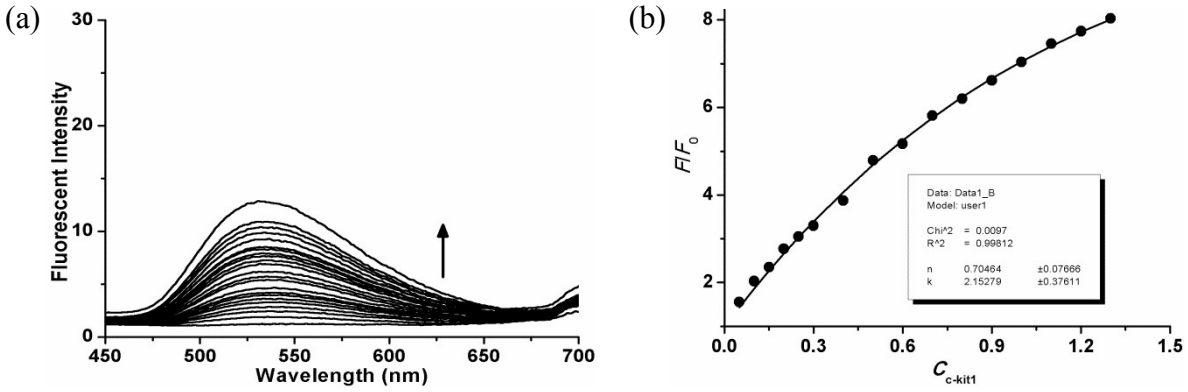

Fig. S14 (a) Fluorescence emission spectra of compound **1a** (0.5 μM) in the presence of c-kit 1 of varying concentrations. (b) Plot of the relative fluorescent intensity (F/F_0) of compound **1a** (0.5 μM) against the concentrations of c-kit 1 in 10 mM Tris-HCl buffer (100 mM KCl, pH 7.0). $\lambda_{ex}/\lambda_{em}$ = 355/530 nm.

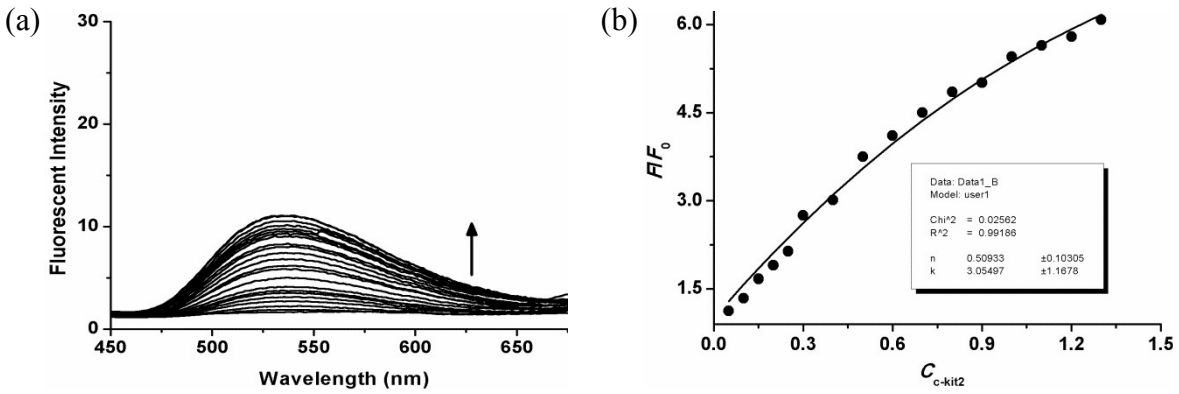

Fig. S15 (a) Fluorescence emission spectra of compound **1a** (0.5 μM) in the presence of c-kit 2 of varying concentrations. (b) Plot of the relative fluorescent intensity (F/F_0) of compound **1a** (0.5 μM) against the concentrations of c-kit 2 in 10 mM Tris-HCl buffer (100 mM KCl, pH 7.0). $\lambda_{ex}/\lambda_{em}$ = 355/530 nm.

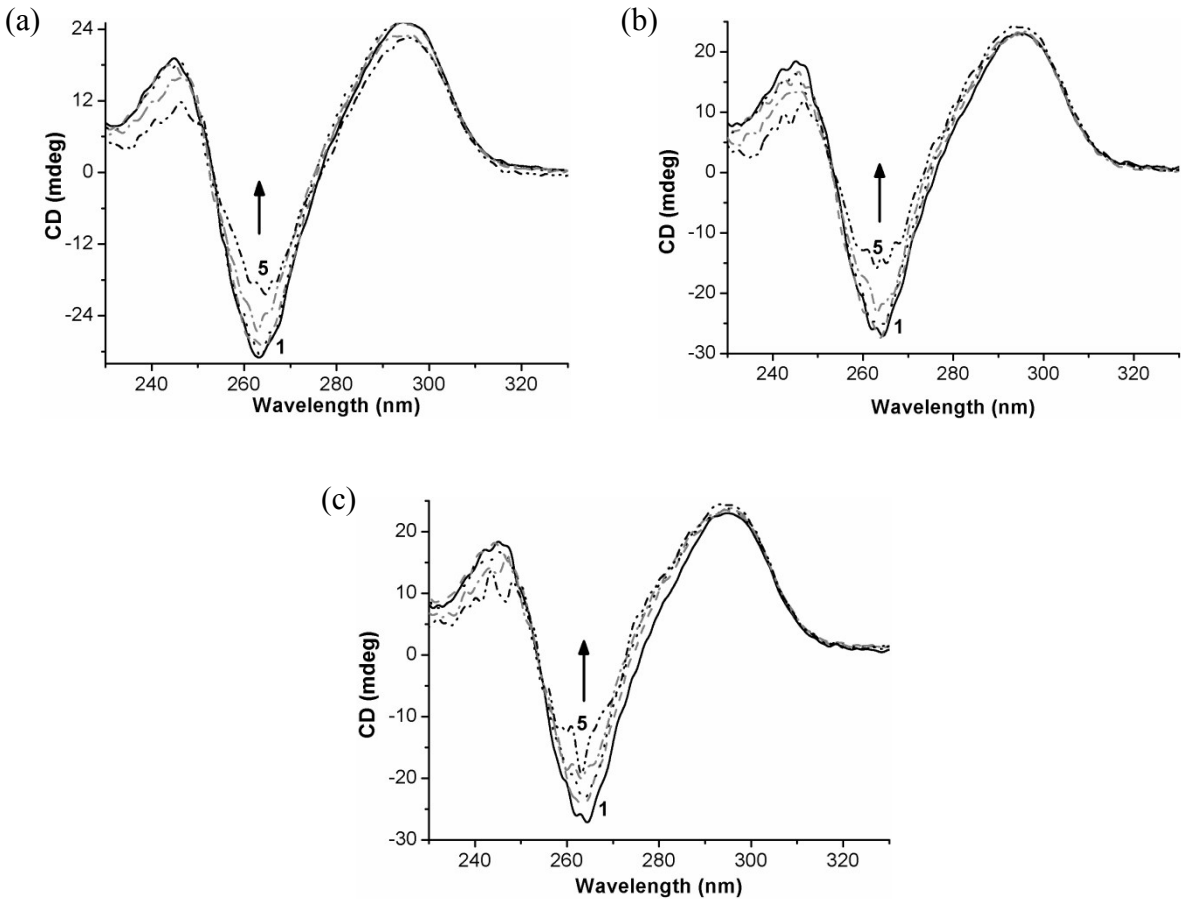

Fig. S16 CD spectra of antiparallel G2T1 (2.5 μM) in 10 mM Tris-HCl and 100 mM NaCl (pH 7.0) with compounds (a) **1a**, (b) **1b** and (c) **1c**: (1) 0 equiv, (2) 1 equiv, (3) 2 equiv, (4) 4 equiv and (5) 8 equiv.

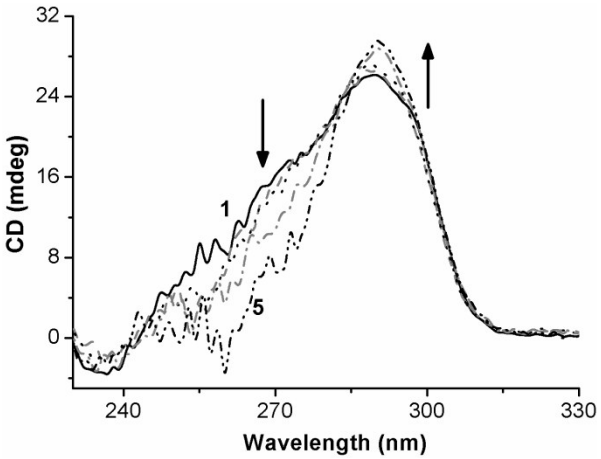

Fig. S17 CD spectra of mixed-type G2T1 (2.5 μM) in 10 mM Tris-HCl and 100 mM KCl (pH 7.0) with compound **1c**: (1) 0 equiv, (2) 1 equiv, (3) 2 equiv, (4) 4 equiv and (5) 8 equiv.

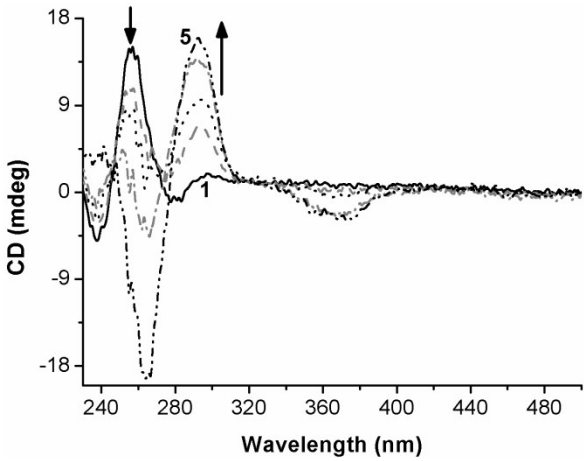

Fig. S18 CD spectra of nonannealed G2T1 (2.5 μM) in 10 mM Tris-HCl (pH 7.0) in the presence of compound **1b**: (1) 0 equiv, (2) 1 equiv, (3) 2 equiv, (4) 4 equiv and (5) 8 equiv.

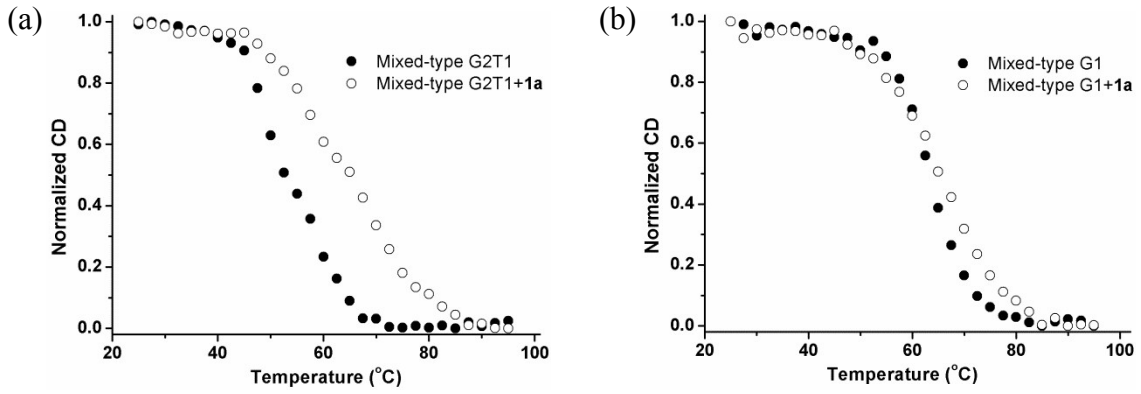

Fig. S19 CD melting profiles at 290 nm for mixed-type G2T1 (3.0 μM, a) and mixed-type G1 (6.0 μM, b) in 10 mM Tris-HCl and 100 mM KCl (pH 7.0) in the presences of compound **1a** with the different concentrations 0 and 12 μM, respectively.

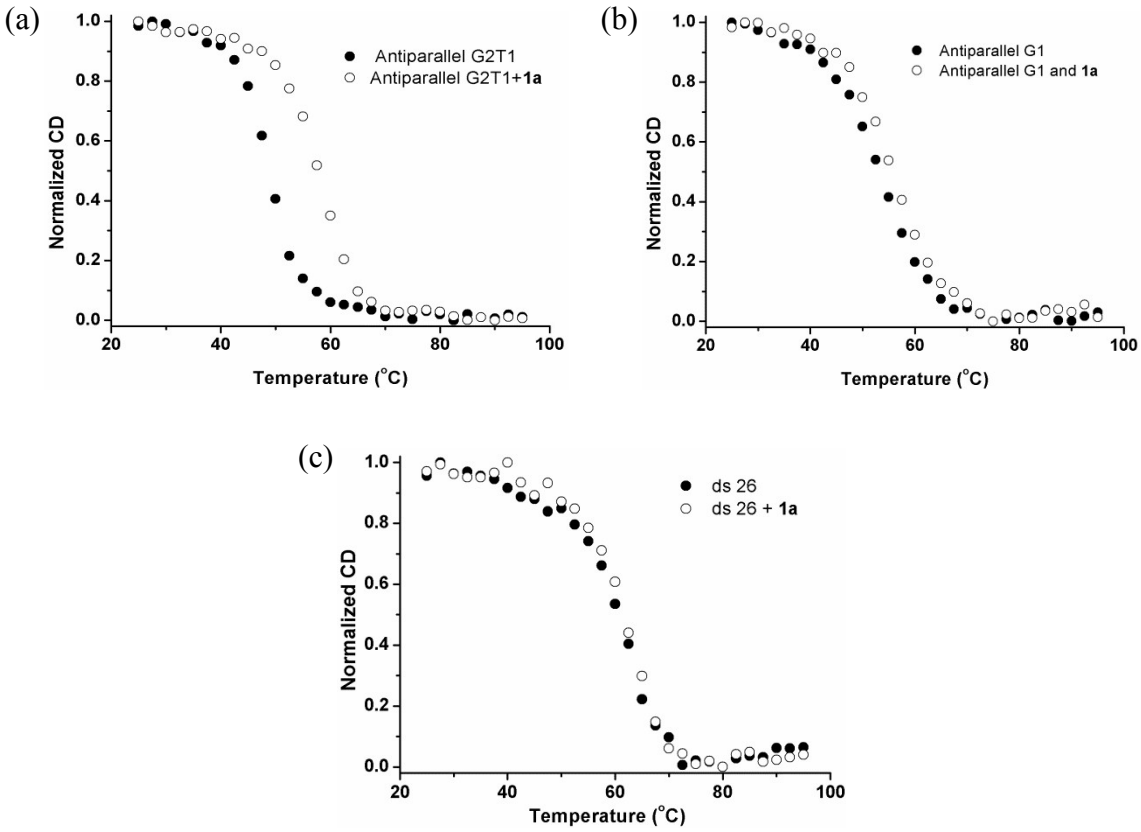

Fig. S20 CD melting profiles at 295 nm for antiparallel G2T1 (3.0 μM, a) and antiparallel G1 (6.0 μM, b), and at 275 nm for ds DNA (3.0 μM, c) in 10 mM Tris-HCl and 100 mM KCl (pH 7.0) in the presences of compound **1a** with the different concentrations 0 and 12 μM,

respectively.